NO Electroreduction

Deutsche Ausgabe: DOI: 10.1002/ange.201502104
Internationale Ausgabe: DOI: 10.1002/anie.201502104

Elucidation of Pathways for NO Electroreduction on Pt(111) from First Principles**

*Andre Clayborne, Hee-Joon Chun, Rees B. Rankin, and Jeff Greeley**

Abstract: *The mechanism of nitric oxide electroreduction on Pt(111) is investigated using a combination of first principles calculations and electrokinetic rate theories. Barriers for chemical cleavage of N–O bonds on Pt(111) are found to be inaccessibly high at room temperature, implying that explicit electrochemical steps, along with the aqueous environment, play important roles in the experimentally observed formation of ammonia. Use of explicit water models, and associated determination of potential-dependent barriers based on Bulter–Volmer kinetics, demonstrate that ammonia is produced through a series of water-assisted protonation and bond dissociation steps at modest voltages (< 0.3 V). In addition, the analysis sheds light on the poorly understood formation mechanism of nitrous oxide (N_2O) at higher potentials, which suggests that N_2O is not produced through a Langmuir–Hinshelwood mechanism; rather, its formation is facilitated through an Eley–Rideal-type process.*

Electroreduction of nitrates, nitrites, and nitric oxide (NO) on platinum electrodes has attracted considerable interest in recent years due to the environmental,[1,2a] biological,[1,2b] and industrial implications of these chemistries.[1] In particular, investigations of the electrochemical reduction of NO and nitrates on Pt-based electrodes have been an important focus of fundamental experimental studies.[3–9] The main products of NO electroreduction on single-crystal platinum electrode surfaces are ammonia (NH_3/NH_4^+), dinitrogen (N_2), and nitrous oxide (N_2O) (Figure 1).[1] For reductive stripping at modest coverages (< 0.45 ML; ML = monolayer) and relatively low potentials (< 0.4 V_{SHE}), it has been well-established that ammonia is produced:

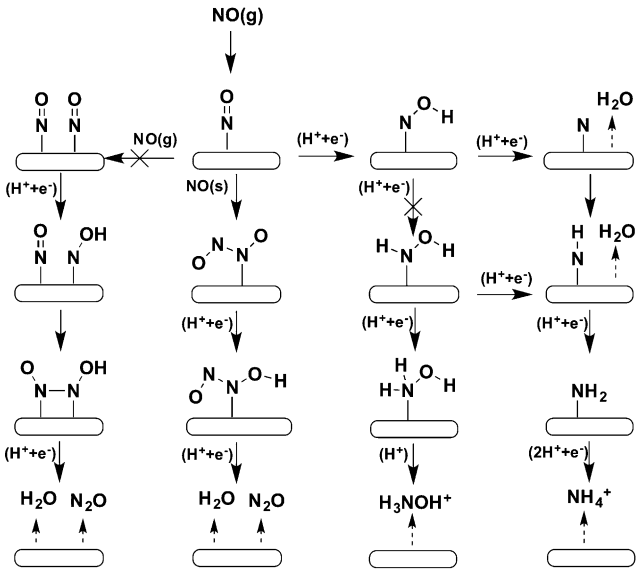

Figure 1. Selected reaction pathways for NO electroreduction on Pt(111) electrodes producing nitrous oxide (N_2O), hydroxylamine (NH_3OH^+), and ammonia (NH_4^+). Arrows with × mark the unfavorable pathways for N_2O and NH_4^+ products, respectively, at low to medium coverages. Dashed arrows indicate products that are released from the surface.

$$NO(g) + 5\,e^- + 6\,H^+ \rightarrow NH_4^+ + H_2O(l) \quad (1)$$

Under continuous reduction conditions, however, N_2O can also be produced at potentials higher than 0.4 V_{SHE} through the overall reaction[5,9]

$$2\,NO(g) + 2\,e^- + 2\,H^+ \rightarrow N_2O(g) + H_2O(l) \quad (2)$$

In spite of these efforts, however, and although NO is considered to be a crucial intermediate in the reduction of both nitrites and nitrates,[10] the exact mechanism of its conversion to the various products remains unclear. For example, concerning ammonia formation, Koper and Beltramo suggested that ammonia is formed through the HNO and H_2NO intermediates, NO→HNO→H_2NO→NH_4^+ + H_2O (concerted proton/electron transfer is implied). In contrast, Cuesta and Escudero suggested that NO→NOH-(HNO)→HNOH→$NH_4^+ + H_2O$ is the favored pathway.[4,5]

[*] Dr. A. Clayborne[+]
Department of Chemistry, Nanoscience Center
University of Jyväskylä
Survontie 9C, Jyväskylä (Finland)
H.-J. Chun,[+] Prof. J. Greeley
School of Chemical Engineering, Purdue University
480 Stadium Mall Drive, West Lafayette, IN (USA)
E-mail: jgreeley@purdue.edu
Prof. R. B. Rankin
Department of Chemical Engineering, Villanova University
White Hall, 800 Lancaster Avenue, Villanova, PA (USA)
[+] These authors contributed equally to this work.

[**] H.-J.C. and J.G. acknowledge funding through a Department of Energy Early Career award through the Office of Science, Office of Basic Energy Sciences, Chemical Sciences, Geosciences, and Biosciences Division. A.C. acknowledges the Academy of Finland for funding. A.C. was formerly at Argonne National Laboratory. Use of the Center for Nanoscale Materials was supported by the U. S. Department of Energy, Office of Science, Office of Basic Energy Sciences, under Contract No: DE-AC02-06CH11357.

Supporting information for this article (calculations performed within the framework of DFT, as implemented in VASP)[19] is available on the WWW under http://dx.doi.org/10.1002/anie.201502104.

Interestingly, although the mechanistic pathways differ, both of these mechanisms suggest an (electro)chemical step for N–O bond activation, a hypothesis that will be further evaluated below. Concerning N_2O formation, early studies on platinum suggested that in order to form N_2O, N–N bonds could form by a Langmuir–Hinshelwood (L-H) mechanism, yielding dimers such as ON–NO, NOH–NO, and HON–NOH, and eventually leading to formation of N_2O.[7] Koper and co-workers, in contrast, proposed an Eley–Rideal-like (E-R) mechanism, whereby a solvated NO could form $(NO)_2$ and eventually produce N_2O.[3]

Here we present mechanisms that elucidate and reconcile experimental observations concerning both NH_3 and N_2O formation on the Pt(111) surface. We employ periodic density functional theory (DFT) calculations and determine potential-dependent free energies using the computational hydrogen electrode model, which has provided excellent descriptions of electroreduction of small molecules, such as oxygen and carbon monoxide (CO), on transition metal surfaces.[11–13] The effect of water on the reaction thermodynamics is determined through ab initio molecular dynamics simulations, while the corresponding effect on kinetics is estimated with sub-bilayer water models. To further investigate the kinetics of the elementary steps, we use a method within the Butler–Volmer formalism to estimate potential-dependent activation free energy barriers.[13] Additional details on the computational methods are provided in the Supporting Information (SI).

Reduction of NO on the Pt(111) electrode involves a multitude of possible intermediates and products, and the thermodynamically most stable configurations of all such species have been analyzed in this work. At low coverages (about 0.1 ML), we find the minimum energy configurations to be generally in agreement with existing experimental and theoretical literature (see the SI for geometries and energetics).[14,15] The most energetically favorable intermediates associated with the hydrogenation steps, based on calculated free energies, are the NOH and HNOH species, as compared to HNO and H_2NO. At a potential of 0.00 V_{SHE}, all free energies of these elementary steps are approximately downhill (Figure 2), suggesting that the onset potential for the reaction will be close to this value, in agreement with numerous experimental observations.

In addition to electrochemical hydrogenation, N–O bond activation is likely to be a central process in the overall NO electroreduction network. Activation barriers for chemical N–O bond dissociation for all considered intermediates are reported in the SI. It is well known that the dissociation barrier for NO itself on Pt(111) is quite high, on the order of 2.3 eV, which is impossible to overcome under electrochemical conditions.[14,15] The activation barrier to break the N–O bond for NOH* is considerably lower (0.9 eV), and upon further hydrogenation, the barrier for HNOH* dissociation is further reduced to approximately 0.7 eV. However, at room temperature, such barriers are still not trivial to overcome, suggesting that other mechanisms explicitly involving the effect of the aqueous solvent and electrochemical charge transfer may be responsible for the observed production of ammonium ions from NO reduction. To further evaluate this possibility, we examine closely the role of water on the activation barriers for the various elementary steps.

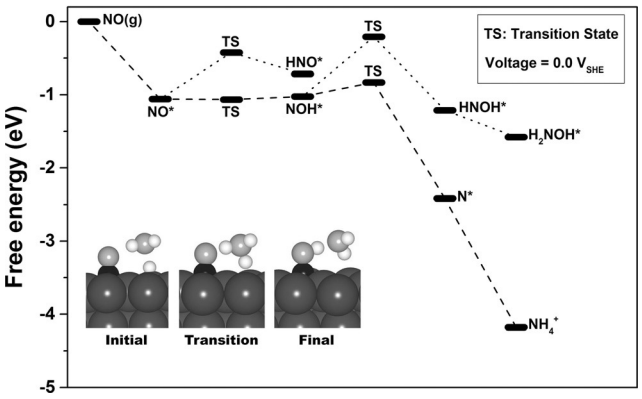

Figure 2. Free energy diagram for NO reduction at 0.11 ML of NO coverage (0.0 V_{SHE}). Large dashes represent the preferred pathway. The inset illustrates the side views of the initial, transition, and final state for the water shuttling protonation of NOH* to form an additional water molecule and N*. Dark gray circles denote Pt, light gray denotes O, black denotes N, and white denotes H.

Activation barriers for coupled proton/electron transfer, together with N–O bond activation in the associated intermediates, are investigated by examining hydrogen shuttling from the surface to the intermediate through a water molecule, as well as direct hydrogen transfer to the intermediates from the surface, as previously described by Janik and co-workers[13] (see the SI). It is interesting to note that, similar to the case of CO_2 reduction, we find that for all O–H forming reactions (including water formation), the activation barrier is lower in the case of hydrogen shuttling, which can be attributed to the polar nature of the O–H bond.[13] These barriers can be associated with a potential scale (SI), and for elementary steps where water can form directly as a result of the coupled proton/electron transfer, N–O bond activation is, in general, relatively facile. Indeed, the barriers of these quasi-concerted processes are often much lower than the corresponding barriers for chemical dissociation of N-O-type bonds (SI, Figure S5), demonstrating that the aqueous environment and associated electrochemical steps play a key role in N–O activation and ammonia formation. We note that the energetic pathways depicted in Figure 2 provide robust understanding of reaction mechanisms but do not necessarily yield quantitative predictions of absolute reaction rates; this point is extensively discussed in the SI.

Based on these considerations, the process for NO electroreduction at low coverage, leading to ammonia formation, can be described as follows. After NO is adsorbed on the surface, protonation leads to the formation of NOH*, which is in turn followed by two simultaneous steps: O–H bond-formation and N–O dissociation, yielding N* and $H_2O(l)$. The remaining surface-bound nitrogen atom then reacts with additional proton/electron pairs to form ammonia. The reaction steps for the process are

$$^* + NO(g) \rightarrow NO^* \quad (3)$$

$$NO^* + H^+ + e^- \rightarrow NOH^* \quad (4)$$

$$NOH^* + H^+ + e^- \rightarrow N^* + H_2O(l) \quad (5)$$

$$N^* + 4H^+ + 3e^- \rightarrow NH_4^+(l) + * \quad (6)$$

As mentioned briefly above, experiments have observed that the primary product for electrochemical reduction of NO is NH_3/NH_4^+ at coverages up to 0.5 ML and potentials less than 0.4 V. Additionally, it has been suggested that, in the case of reductive stripping, the observed voltammetric features are a result of NO* occupying different sites on the Pt(111) surface, with the higher voltage peaks corresponding to stripping from top sites and the lowest voltage peaks being associated with NO at threefold sites.[5–7] Recent DFT calculations by Mavrikakis and co-workers[15] have indirectly supported this argument, demonstrating that, with increasing coverage, NO will occupy both three-fold and top sites, with high coverage NO showing higher barriers to chemical N–O bond activation. The mechanism discussed above is generally consistent with these observations and corresponds directly to the lower voltage peaks observed in the stripping experiments. Additional calculations performed at 0.5 ML coverages, with NO occupying both top and fcc sites, do indeed suggest that HNO* formation now occurs at top sites with more favorable thermodynamics and kinetics (see also SI), but formation of NOH* at threefold sites also continues to be a favorable pathway.

Additional effects of higher NO coverages can be observed under continuous reduction conditions, which are of practical importance for electrochemical wastewater treatment strategies.[2a] In these conditions, which are characterized by NO-saturated solutions, formation of an additional product, N_2O, has been observed at high potentials. The NO surface coverage, in turn, is relatively high. Given these considerations, we investigated N_2O formation at NO coverages up to 0.45 ML (for comparison, results at lower coverages are reported in the SI). We first probed the possibility of N_2O formation through Langmuir–Hinshelwood reactions to form *cis*-type N–N species between NO* and either hydrogenated NO intermediates or atomic nitrogen, including NO–NOH*, NOH–NOH*, NO–NH*, NO–HNO, and N–NO*. Barriers to form these species are all on the order of 1.0 eV (geometry optimization of other potentially interesting dimeric species, such as NO–NO*, on the flat surface shows no bond formation between the two N atoms). As observed by Mavrikakis and co-workers, such reactions would be plausible under heterogeneous catalytic conditions at higher NO coverages and elevated temperatures,[15] but under electrochemical conditions, they are prohibitive (see the SI for additional details). Furthermore, for such a pathway to be plausible, some form of hydrogenated NO would need to be present on the surface, and our results on the reduction mechanism, described above, strongly suggest that such species are only found at much lower potentials than N_2O is formed. These considerations, in turn, suggest that a traditional Langmuir-Hinshelwood picture is not adequate to explain the observed product distributions, and solution-mediated reactions may, again, play a key role.

To simulate the reaction of solution-phase NO with surface NO, we analysed the kinetics and thermodynamics of the formation of both *trans*- and *cis*-$(NO)_2$ dimers on the Pt(111) surface through the reaction

$$NO_{soln} + NO^* \rightarrow NO{-}NO^* \quad (7)$$

We note, in passing, that reaction of two solution-phase, or otherwise solvated, NO molecules would essentially correspond to an uncatalyzed reaction, and such a process is unlikely to occur under low temperature electrochemical conditions. Formation of the *trans*-$(NO)_2$ dimer, in contrast, is relatively favorable, with an N–N bond formation free energy barrier of 0.7 eV (Figure 3). The formation occurs when

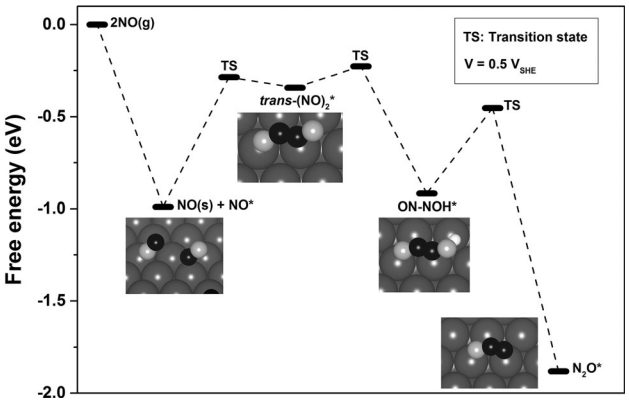

Figure 3. Free energy diagram for NO electroreduction leading to nitrous oxide (N_2O) at 0.5 V_{SHE} ($\theta_{NO} = 0.45$ ML). Images represent angled views of intermediates along the reaction pathway with additional coadsorbed NO molecules removed for clarity. Dark gray circles denote Pt, light gray denotes O, black denotes N, and white denotes H.

a solution-phase NO molecule becomes weakly physisorbed on a Pt top site adjacent to a chemisorbed NO* molecule, while simultaneously forming an N–N bond with this NO*, which is bound to the surface through its N atom. This process cannot occur through a surface-mediated mechanism, as the kinetic barrier to form the *trans*-$(NO)_2$ dimer from two NO* species is 1.40 eV (at low coverage it is even higher, at 2.01 eV). Once the *trans*-$(NO)_2$ dimer is formed, protonation leads to the formation of the NO–NOH* species. This reaction is then followed by a low-barrier, concerted bond formation–dissociation step (Figure 3), resulting in formation of $N_2O(g)$ and an additional H_2O molecule at ca. 0.5 V_{SHE}. The barrier for this step, approximately 0.5 eV, is well below 0.7 eV, which is traditionally considered to be an accessible barrier at room temperature.[16] We note that the NO–NOH* formation barrier is of approximately the same magnitude as the corresponding barrier for the *trans*-dimer to decompose back to separated NO species. Therefore, the forward reaction involving N_2O formation is a competitive pathway, and after the *trans*-dimer formation from Equation (7), the reaction steps are as follows:

$$NO{-}NO^* + H^+ + e^- \rightarrow NO{-}NOH^* \quad (8)$$

$$NO{-}NOH^* + H^+ + e^- \rightarrow N_2O(g) + H_2O(l) + * \quad (9)$$

These results suggest that the formation of N_2O occurs at approximately 0.5 V_{SHE} through reaction of solution-phase NO with NO* to form a *trans*-NO dimer, followed by protonation and proton-assisted water removal. These mechanistic implications are fully consistent with experimental reports showing N_2O formation at an onset potential of 0.4–0.7 V_{RHE} under continuous reduction conditions and with measurements by Koper and co-workers[3a] demonstrating formation of N_2O when NO is found both in solution and on the platinum surface. The present analysis demonstrates that such a reaction can only occur through formation of a *trans*-dimer, wherein one of the reacting NO molecules approaches the surface with its oxygen end down, limiting its binding with the platinum and facilitating reaction with a neighboring, chemisorbed NO molecule (see the SI). NO approaching the surface with the nitrogen atom down, however, is likely to chemisorb before reacting with neighboring NO molecules due to the very strong N–surface interaction. This chemisorption, in turn, leads to higher barriers associated with formation of *cis*-dimers, as described above, making such a mechanism unlikely. Finally, we observe that, although this process is possible at low NO surface coverages (SI), it has the most favorable kinetics at high NO coverages, where weakly bound top site NO is populated and can readily react with solution-phase species.

In conclusion, DFT calculations of the thermodynamic and kinetic barriers of elementary steps have elucidated the reduction mechanism of NO on Pt(111) under electrochemical conditions. The primary path leading to NH_3/NH_4^+ proceeds through the reduction of NO to NOH at lower coverages, which will lead to ammonia through water-assisted hydrogenation of surface bound species. Likewise, N_2O formation does not occur through the formation of NO-dimers through a surface mediated process, but through an Eley–Rideal-type mechanism wherein solvated NO species interact with surface-bound NO molecules to form *trans*-$(NO)_2$, followed by formation of an NO–NOH species and then N_2O. Our proposed pathways underline the importance of the aqueous electrochemical environment in the reduction of NO on electrode surfaces and hint that similar effects could be present in the reduction of other nitrogen species such as nitrates and nitrites,[1,10,17] as well as in the oxidation of ammonia.[18] Extension of these mechanistic insights to related nitrogen-cycle chemistries and alternative catalyst structures may, ultimately, facilitate improved design of nitrogen-cycle catalysts for targeted environmental and synthesis applications.

Keywords: ammonia · density functional theory · electrocatalysis · nitrous oxide · NO reduction

How to cite: *Angew. Chem. Int. Ed.* **2015**, *54*, 8255–8258
Angew. Chem. **2015**, *127*, 8373–8376

[1] V. Rosca, M. Duca, M. T. Groot, M. T. M. Koper, *Chem. Rev.* **2009**, *109*, 2209–2244.
[2] a) J. W. Peel, K. J. Reddy, B. P. Sullivan, J. M. Bowen, *Water Res.* **2003**, *37*, 2512–2519; b) B. J. Privett, J. H. Shin, M. H. Scoenifisch, *Chem. Soc. Rev.* **2010**, *39*, 1925–1935.
[3] a) A. C. A. de Vooys, M. T. M. Koper, R. A. van Santen, J. A. R. van Veen, *Electrochim. Acta* **2001**, *46*, 923–930; b) A. C. A. de Vooys, M. T. M. Koper, R. A. van Santen, J. A. R. van Veen, *J. Catal.* **2001**, *202*, 387–394; c) A. C. A. de Vooys, G. L. Beltramo, B. van Riet, J. A. R. van Veen, M. T. M. Koper, *Electrochim. Acta* **2004**, *49*, 1307–1314.
[4] V. Rosca, G. L. Beltramo, M. T. M. Koper, *Langmuir* **2005**, *21*, 1448–1456.
[5] A. Cuesta, M. Escudero, *Phys. Chem. Chem. Phys.* **2008**, *10*, 3628–3634.
[6] K. Nakata, A. Okubo, K. Shimazu, A. Yamakata, S. Ye, M. Osawa, *Langmuir* **2008**, *24*, 4352–4357.
[7] J. A. Colucci, M. J. Foral, S. H. Langer, *Electrochim. Acta* **1985**, *30*, 521–528.
[8] a) J. Yang, P. Sebastian, M. Duca, T. Hoogenboom, M. T. M. Koper, *Chem. Commun.* **2014**, *50*, 2148–2151; b) M. C. Figueiredo, J. Solla-Gullón, F. J. Vidal-Iglesias, V. Climent, J. M. Feliu, *Catal. Today* **2013**, *202*, 2–11; c) J. Souza-Garcia, E. A. Ticianelli, V. Climent, J. M. Feliu, *Chem. Sci.* **2012**, *3*, 3063–3070.
[9] a) M. C. Figueiredo, V. Climent, J. M. Feliu, *Electrocatalysis* **2011**, *4*, 255–262; b) F. R. Rima, K. Nakata, K. Shimazu, M. Osawa, *J. Phys. Chem. C* **2010**, *114*, 6011–6018.
[10] a) J. Yang, F. Calle-Vallejo, M. Duca, M. T. M. Koper, *ChemCatChem* **2013**, *5*, 1773–1783; b) M. Duca, M. C. Figueiredo, V. Climent, P. Rodriquez, J. M. Feliu, M. T. M. Koper, *J. Am. Chem. Soc.* **2011**, *133*, 10928–10939.
[11] J. K. Nørskov, J. Rossmeisl, A. Logadottir, L. Lindqvist, J. R. Kitchin, T. Bligaard, H. Jonsson, *J. Phys. Chem. B* **2004**, *108*, 17886–17892.
[12] a) J. Greeley, I. E. L. Stephens, A. S. Bondarenko, T. P. Johansson, H. A. Hansen, T. F. Jaramillo, J. Rossmeisl, I. Chorkendorff, J. K. Norskov, *Nat. Chem.* **2009**, *1*, 552–556; b) J. A. Keith, T. Jacob, *Agnew. Chem. Int. Ed.* **2010**, *49*, 9521–9525; *Angew. Chem.* **2010**, *122*, 9711–9716.
[13] X. Nie, M. R. Esopi, M. J. Janik, A. Asthagiri, *Agnew. Chem. Int. Ed.* **2013**, *52*, 2459–2462; *Angew. Chem.* **2013**, *125*, 2519–2522.
[14] a) M. Gajdoš, J. Hafner, A. Eichler, *J. Phys. Condens. Matter* **2006**, *18*, 41–45; b) Z.-H. Zeng, J. Da Silva, H.-Q. Deng, W.-X. Li, *Phys. Rev. B* **2009**, *79*, 205413.
[15] C. A. Farberow, J. A. Dumesic, M. Mavrikakis, *ACS Catal.* **2014**, *4*, 3307–3319.
[16] H. F. Wang, Z. P. Liu, *J. Am. Chem. Soc.* **2008**, *130*, 10996–11004.
[17] J. Yang, F. Calle-Vallejo, M. Duca, M. T. M. Koper, *ChemCatChem* **2013**, *5*, 1773–1783.
[18] N. J. Bunce, D. Bejan, *Electrochim. Acta* **2011**, *56*, 8085–8093.
[19] a) G. Kresse, J. Hafner, *Phys. Rev. B* **1993**, *47*, 558–561; b) G. Kresse, J. Hafner, *Phys. Rev. B* **1994**, *49*, 14251–14269; c) G. Kresse, J. Furthmuller, *Phys. Rev. B* **1996**, *54*, 11169–11186; d) G. Kresse, J. Furthmuller, *Comput. Mater. Sci.* **1996**, *6*, 15–50.

Received: March 5, 2015
Published online: June 5, 2015